Facile Method for Modulating the Profiles and Periods of Self-Ordered Three-Dimensional Alumina Taper-Nanopores

ARTICLE *in* ACS APPLIED MATERIALS & INTERFACES · SEPTEMBER 2012

Impact Factor: 6.72 · DOI: 10.1021/am301603e · Source: PubMed

7 AUTHORS, INCLUDING:

Juan Li
Chinese Academy of Sciences
65 PUBLICATIONS **768** CITATIONS
SEE PROFILE

Cheng Chen
University of Portsmouth
23 PUBLICATIONS **167** CITATIONS
SEE PROFILE

Qingli Hao
Nanjing University of Science and Technology
88 PUBLICATIONS **2,074** CITATIONS
SEE PROFILE

Xuefeng Gao
Chinese Academy of Sciences
34 PUBLICATIONS **3,615** CITATIONS
SEE PROFILE

ACS APPLIED MATERIALS & INTERFACES

Research Article

www.acsami.org

Facile Method for Modulating the Profiles and Periods of Self-Ordered Three-Dimensional Alumina Taper-Nanopores

Juan Li,[†,‡] Congshan Li,[†,‡] Cheng Chen,[†,‡] Qingli Hao,[§] Zhijia Wang,[†,§] Jie Zhu,[†] and Xuefeng Gao*[,†]

[†]Suzhou Institute of Nano-Tech and Nano-Bionics, Chinese Academy of Sciences, Suzhou 215123, P. R. China

[‡]Graduate University of the Chinese Academy of Sciences, Beijing 100049, P. R. China

[§]School of Chemical Engineering, Nanjing University of Science and Technology, Nanjing 210094, P. R. China

Supporting Information

ABSTRACT: We report a facile nanofabrication method, one-step hard anodizing and etching peeling (OS-HA-EP) of aluminum foils followed by multistep mild anodizing and etching pore-widening (MS-MA-EW), for the controllable tailoring of hexagonally packed three-dimensional alumina taper-nanopores. Their profiles can be precisely tailored by the synergistic control of anodizing time, etching time and cyclic times at the MS-MA-EW stage, exemplified by linear cones, whorl-embedded cones, funnels, pencils, parabolas, and trumpets. Meantime, their periods can also be modulated in the range of 70−370 nm by choosing matched anodizing electrolytes (e.g., $H_2C_2O_4$, H_2SO_4, $H_2C_2O_4$−H_2SO_4, and $H_2C_2O_4$−C_2H_5OH mixture) and anodizing voltages at the OS-HA-EP stage. We also demonstrated that the long-range ordering of nanopits and the peak voltage of stable self-ordered HA, which are unachievable in a single $H_2C_2O_4$ electrolyte system, can be effectively tuned by simply adding tiny quantity of H_2SO_4 and C_2H_5OH to keep an appropriate HA current density, respectively. This method of using the combination of simple pure chemical nanofabrication technologies is very facile and efficient in realizing the controllable tailoring of large-area alumina membranes containing self-ordered taper-nanopores. Our work opens a door for exploring the novel physical and chemical properties of different materials of nanotaper arrays.

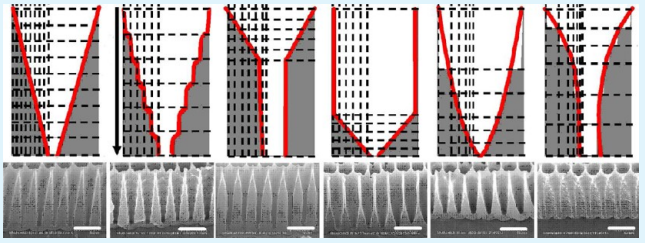

KEYWORDS: *taper-nanopore, alumina membrane, anodizing, etching, combined chemistry*

INTRODUCTION

Very recently, a type of emerging anodic alumina membranes containing ordered taper-nanopore arrays (OTNPAs) attracted intensive interest because of its unique potential in developing bionic broadband antireflection, dry-style antifogging and self-cleaning nanomaterials,[1−6] nanofluidic energy-conversion devices,[7−10] SERS-based sensors,[11,12] oriented growth of mesochannels,[13−16] and so on.[17−22] It should be pointed out that the alumina OTNPA structures are a type of very crucial hard templates for the controllable fabrication and property research of different materials (especially metal and polymer) of three-dimensional (3D) nanotaper (e.g., tapered nanonipple,[2−6] nanocone[12,17,18] and nanopore[21]) arrays. However, their geometrical parameters are very hard to modulate in a facile and efficient way at this stage, which seriously impedes the proceeding of related researches. To date, only the conical OTNPAs with limited periods can be achieved by the multistep mild anodizing and etching pore-widening (MS-MA-EW) of aluminum (Al) foils, prepatterned by one-step mild anodizing and etching peeling[5] and mechanical imprinting of period-tunable SiC molds[22,23] and monolayer SiO_2 nanospheres.[24] However, the existing methods have respectively inherent disadvantages: the first is too time-consuming (>8 h) and period-fixed (e.g., 100 nm for oxalic acid at 40 V); the second is costly and unavailable to most researchers; the third is not so easy to operate for samples with larger area (e.g., several centimeters) or periods <150 nm. Besides, the precise tailoring of taper-nanopores with other complex profiles is still unreported hitherto.[6] Therefore, it is a great challenge to find a facile and efficient method for tailoring 3D OTNPA stuctures with controllable and tunable geometrical parameters.

Because the complex 3D OTNPA structures are very hard to obtain by any single top-down or bottom-up nanofabrication method, it may be the only choice to adopt the combination of multiple facile and efficient nanofabrication technologies at this stage. Compared with top-down technologies, pure chemical methods are ideal due to their inherent merits in the fabrication cost, operation simplicity and equipment availability. Inspired from recently developed hard anodizing technologies,[25−31] characterized by rapid oxide growth (~1×10^3 nm/min), tunable periods and long-range ordering, we propose that one-step hard anodizing and etching peeling (OS-HA-EP) may be an ideal self-ordered nanopit patterning technology, which has not been applied for the fabrication of 3D OTNPAs hitherto.

Received: August 9, 2012
Accepted: September 28, 2012
Published: September 28, 2012

   dx.doi.org/10.1021/am301603e | *ACS Appl. Mater. Interfaces* 2012, 4, 5678−5683

Here, we report the controllable tailoring of 3D OTNPA structures by the combined OS-HA-EP and MS-MA-EW, dispensing with any aid of external physical processes or any costly and/or unavailable equipment. By choosing matched electrolytes and reaction parameters, we can not only tailor a series of complex 3D taper-nanopores with predesigned profiles, exemplified by linear cones, whorl-embedded cones, funnels, pencils, parabolas and trumpets, but also tune their periods in a broader range (70−370 nm). The basic tailoring principles and relationships between the geometrical parameters and reaction conditions under different electrolyte systems (e.g., $H_2C_2O_4$, $H_2C_2O_4$−H_2SO_4 and $H_2C_2O_4$−C_2H_5OH mixture) have been well revealed. Although the used electrochemical anodizing and chemical etching technologies are very simple and well-established, their smart combination for realizing the low-cost and large-area tailoring of 3D OTNPAs is innovative and, importantly, very effective.

EXPERIMENTAL SECTION

Patterning of Self-Ordered Nanopits by the OS-HA-EP. The electropolished highly pure Al foils (99.999%) were placed in an electrochemical cell with a circle cooling system, where the cooling liquid (ethanol) is in thermal contact with the Al substrate to remove the reaction heat. Electrolyte solutions are set at 0−1 °C. For 0.3 M oxalic acid, anodization first proceeded at 40 V for 8 min and then the voltage was gradually increased to the target value (120−150 V) at the rate of 0.5 V s^{-1} (0.25 V s^{-1} for 160 V). For 0.3 M sulfuric acid, anodization was performed at 25 V for 8 min, followed by increasing the voltage at 0.1 V s^{-1} until the target value. For a mixture of oxalic acid (0.3 M) and sulfuric acid (0.001 to 0.08 M), the anodization was first conducted at 35 V for 8 min, followed by increasing the voltage at 0.5 V s^{-1} until the target value. For a mixture of oxalic acid (0.3 M) and ethanol (0.34 M), anodization first proceeded at 40 V for 8 min and then the voltage was gradually increased to the target value (160−180 V) at the rate of 0.5 V s^{-1}. During the anodization, all electrolyte solutions were vigorously stirred and the total anodizing time was 1.5 h. Finally, hexagonally packed nanopit pattern was left on the surface after the removal of porous alumina layer via immersing the samples into a mixed solution of 1.8 wt % CrO_3 and 6 wt % H_3PO_4 at 65 °C for 3 h.

In situ Growth of Taper-Nanopores by the MS-MA-EW. The cyclic times are dependent on the complexity of predesigned profiles. The each-step mild anodization was conducted in 0.29 M H_3PO_4 (0.3 M $H_2C_2O_4$) at 10 °C (17 °C), the anodizing voltage was chosen according to the empirical rules $U_{MA} = D_{int}/2.5$ ($U_{MA} = D_{int}/2$). The anodizing time was determined by the depth of the predesigned taper-nanopores, adjustable between 20 and 250 s. The corresponding pore-widening treatment was performed by immersing the samples in 0.43 M H_3PO_4 (30 °C) for different etching time (0 to 30 min).

Characterization. The geometrical morphologies of all samples were observed under a field-emission scanning electron microscope (FE-SEM, Hitachi S-4800) after sputtering a 15-nm thickness of Au layer.

RESULTS AND DISCUSSION

Figure 1a-c shows the schematic of tailoring the OTNPA structures. The combined OS-HA-EP and MS-MA-EW reactions are responsible for the prepatterning of Al foils and the in situ growth of taper-nanopores, respectively. To carry out the in situ growth of taper-nanopores at the sites of self-ordered nanopits, generated at the OS-HA-EP stage, the anodizing voltage U_{MA} at the MS-MA-EW stage should meet the following expression

$$U_{MA} = \frac{D_{int}}{X_{MA}} = \left(\frac{X_{HA}}{X_{MA}}\right)U_{HA}$$

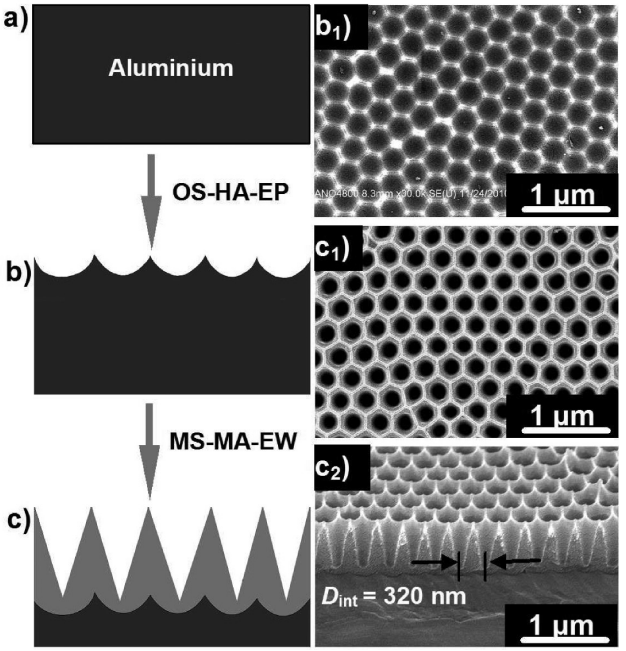

Figure 1. (a−c) Schematic of tailoring hexagonally packed taper-nanopores. (b_1) SEM Top-view of the as-prepared self-ordered nanopit pattern. (c_1, c_2) SEM top-view and side-view of the in situ grown taper-nanopores with average interpore distance of 320 nm.

where D_{int} is the period (interpore distance) of ordered nanopits and in situ grown taper-nanopores; U_{HA} is the self-ordered HA voltage; X_{HA} and X_{MA} are the proportionality constant (PC) of HA and MA in specific electrolytes, respectively.[25] In principle, the D_{int} is decided by the U_{HA}, which is closely related to the applied electrolyte ingredients, whereas the profiles of taper-nanopores can be tailored by the synergistic combination of anodizing time t_{MA}, etching time t_{EW}, and cyclic times T.

Just as expected, the 3D OTNPA structures can be efficiently tailored by the smart combination of the OS-HA-EP and MS-MA-EW. Exemplified by a 0.3 M oxalic acid, a hexagonally packed nanopit pattern (Figure $1b_1$), with average D_{int} ~320 nm and domain sizes 4−5 μm, can be obtained easily by the HA reaction for 1.5 h at 150 V followed by the EP treatment. However, performing the same time of OS-MA-EP only can obtain less ordered nanopits with D_{int} ~100 nm and domain sizes less than 1 μm (see Figure S1 in the Supporting Information). In fact, to obtain the highly ordered nanopits, the MA reaction must last for far more than 8 h, even several days, where the achieved domain size is only 1.5−2 μm.[32,33] It was found that the pore growth rate (1144 nm/min) of HA is far higher than that of MA (108 nm/min), which is the just reason of inducing the long-range self-ordering in a shorter time.[25] Then, at a matched MS-MA-EW condition (U_{MA} = 128 V, t_{MA} = 100 s, t_{EW} = 20 min, T = 5), these nanopits can induce the situ growth of conical nanopores. From their scanning electron microscopic (SEM) top-view (Figure $1c_1$) and side-view (Figure $1c_2$), we can easily obtain an average interpore distance of 320 nm, depth of 480 nm and cone angle of 31.8°. In our preliminary experiments, a 2-in. disk of sample can be reproducibly fabricated (see Figure S2 in the Supporting Information), having the uniformly distributed conical nanopores at the whole surface. Because of the industry-compatible nature, we suppose that such combined method has the

dx.doi.org/10.1021/am301603e | ACS Appl. Mater. Interfaces 2012, 4, 5678−5683

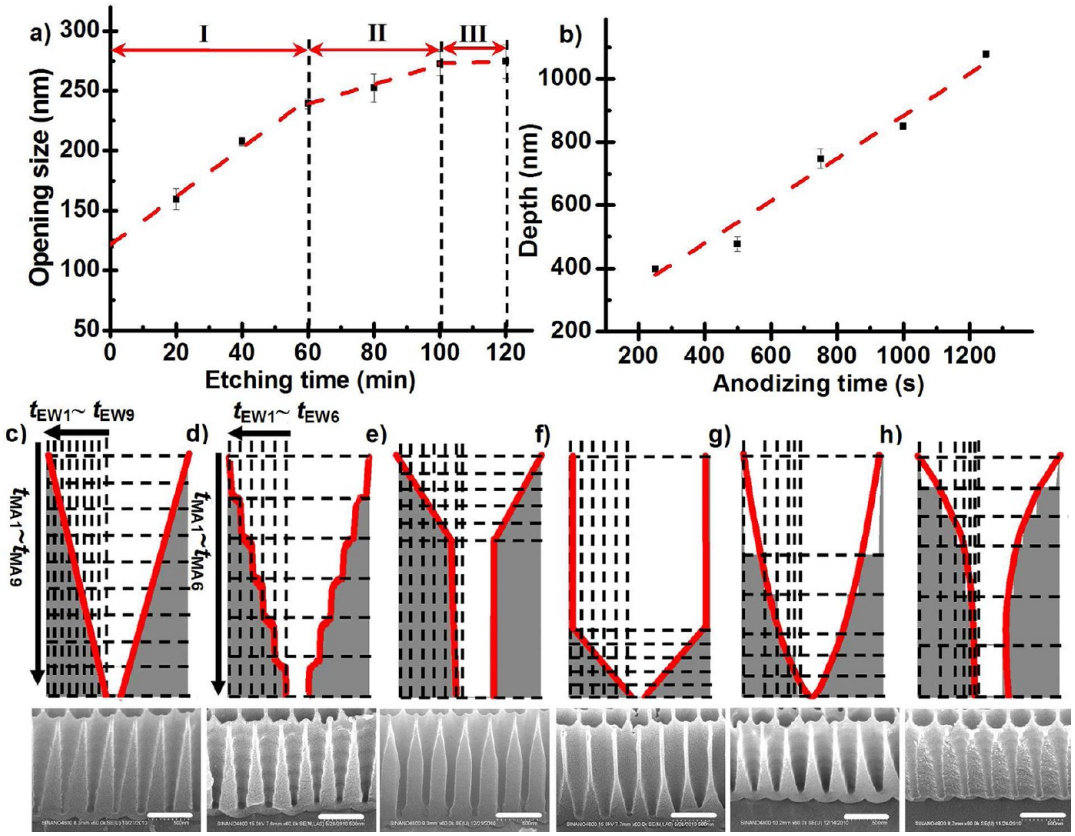

Figure 2. (a) Opening sizes of conical nanopores varied with the total etching time. (b) Depths of conical nanopores varied with the total anodizing time. (c–h) Diverse profiles of taper-nanopores (the bottom) can be tailored on the basis of their predesigned sectional drawings (the top), exemplified by a (c) linear cone, (d) whorl-embedded cone, (e) funnel, (f) pencil, (g) parabola, and (h) trumpet. The scale bars: 500 nm.

potential to evolve into be a practical nanofabrication technique.

To realize the precise profile tailoring of taper-nanopores, it is essential to grasp their etching and growth dynamics. By fixing other reaction conditions constant (U_{MA} = 128 V, t_{MA} = 200 s, T = 5), we first explore the opening sizes of conical nanopores varied with total etching time, as shown in Figure 2a. It is evident that the etching dynamics curve presents three distinct stages, accompanying by the pore-widening rate reducing from 2 nm/min (stage I) down to 0.9 nm/min (stage II), finally close to zero (stage III). This is ascribed to the difference of etching rate between the wall inner and outer. The thicker anion-containing outer corrodes relatively easy while the thinner anion-free inner at the cell border is hard to solve.[34,35] In this system, controlling total etching time in the range of 80–100 min is appropriate and the longitudinal growth of taper-nanopores is almost fully decided by the anodizing time, unaffected by inserted etching.[34] We further study the depths of taper-nanopores varied with total anodizing time by fixing other parameters constant (U_{MA} = 128 V, t_{EW} = 20 min, T = 5). As shown in Figure 2b, the depth of taper-nanopores linearly increases with the total anodizing time, where their growth rate is caculated to be 0.67 nm/s.

After grasping the etching and growth rates, we can control the reaction parameters, t_{MA}, t_{EW}, and T, to tailor the desired profiles of OTNPAs. As shown in the insets of Figure 2c–h, we can divide the transverse size and longitudinal depth of cross sections of predefined taper-nanopores into multiple segments via simply drawing vertical and horizontal lines at chosen data points and thus determine the corresponding t_{MA} and t_{EW} at each MA and EW step. The chosen data point numbers (that is, the cyclic times T) should not be less than 5, among which the upper vertex, lower vertex, and mutant sites at the profile lines are required. In general, the more the acquisition data points, the higher the quality of the tailored profiles. For example, to obtain higher-quality conical nanopores (Figure 2c), we may adopt the strategy of reducing t_{MA} and t_{EW} and adding T (e.g., t_{MA} = 135 s, t_{EW} = 11 min, T = 9). To obtain the conical nanopores embedded with whorls (Figure 2d), we may add t_{MA} and t_{EW} (e.g., t_{MA} = 200 s, t_{EW} = 20 min, T = 6) to produce discontinuous joints between segments, where the whorl number is decided by T. To obtain the composite geometries consisting of cylindrical and conical nanopores, we may add one-step anodizing before or after the MS-MA-EW. Figure 2e shows arrays of funnel-shaped nanopores that can be tailored at conditions: t_{MA1-5} = 80 s, t_{MA6} = 800 s, t_{EW1-5} = 18 min, t_{EW6} = 10 min. Similarly, the pencil-shaped nanopores (Figure 2f) can be tailored at matched conditions: t_{MA1} = 800 s, t_{MA2-6} = 80 s, t_{EW1} = 10 min, t_{EW2-5} = 22.5 min, t_{EW6} = 0 min. To tailor complex nonlinear taper-nanopores, we can adjust t_{MA} and t_{EW} nonuniformly. For the parabola-shaped nanopores (Figure 2g), it is proper to adopt t_{MA1} = 400 s, t_{MA2-3} = 160 s, t_{MA4-6} = 80 s, t_{EW1} = 30 min, t_{EW2-3} = 20 min, t_{EW4-5} = 15 min, t_{EW6} = 0 min. Figure 2h shows the trumpet-shaped nanopores tailored at the conditions: t_{MA1-3} = 120 s, t_{MA4-6} = 200 s, t_{EW1} = 30 min, t_{EW2} = 25 min, t_{EW3} = 15 min, t_{EW4} =10 min, t_{EW5} = 8 min, t_{EW6} = 7 min. Clearly, the tailoring of the OTNPAs is based on the synergetic control of the longitudinal growth of pores, the lateral etching of pore walls and their each-step match with the scallop shape of pore bottom. So precise profile tailoring ability

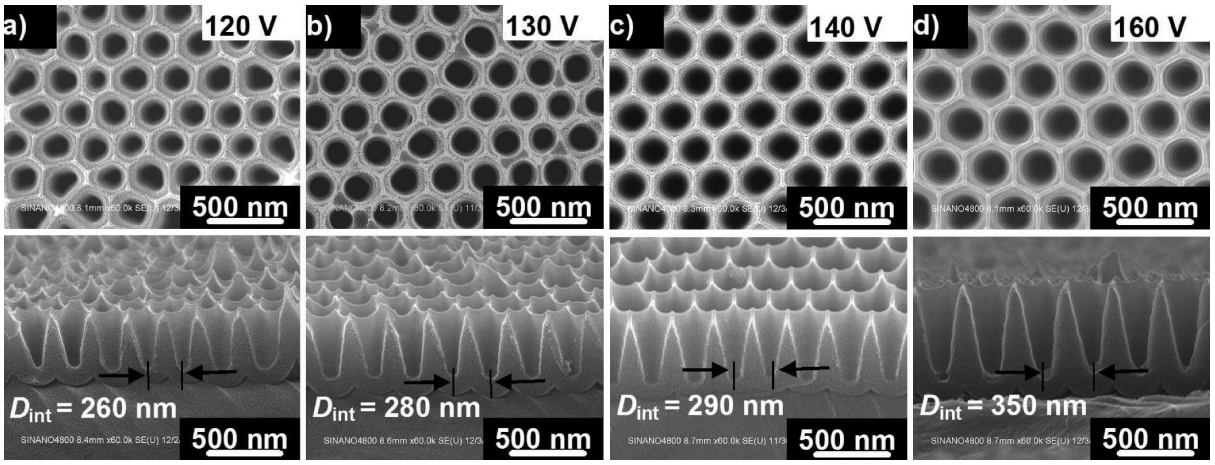

Figure 3. SEM top-views and side-views of self-ordered conical nanopore arrays with tunable interpore distance: 260, 280, 290, and 350 nm, which corresponds to the anodizing voltage of 120, 130, 140, and 160 V at the MS-HA-EW stage. The adopted electrolyte is 0.3 M oxalic acid.

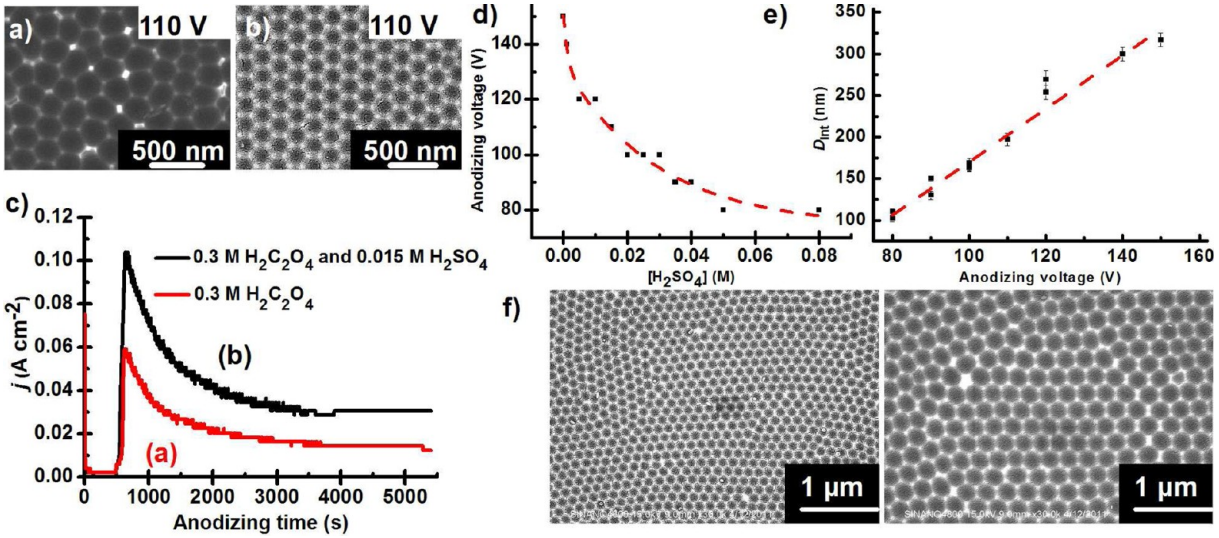

Figure 4. Contrast of SEM images of the nanopit pattern as-prepared (a) before and (b) after adding a tiny quantity of H_2SO_4 in the $H_2C_2O_4$ electrolyte system, where the anodizing voltages (110 V) are kept the same. The corresponding current−time transients are given in panel *c*. Clearly, the current density can be greatly enhanced by the tiny adding of H_2SO_4. (d) Sustainable maximum anodizing voltages U_{HA} as a function of $[H_2SO_4]$. (e) Corresponding periods D_{int} of self-ordered nanopits as a function of the maximum U_{HA}. f) Two examples of tailored nanopit patterns with predefined periods: 130 and 236 nm, which can designate reaction conditions according to the work curves. The actually obtained periods are 128.5 ± 5.1 nm (left) and 238.1 ± 8.2 nm (right), which agree well with the predefined values.

at the 3D scale is unprecedented and also unachievable by conventional top-down nanofabrication technologies.

Remarkably, this method can also easily tune the periods of the OTNPA structures because there exists a broader range of self-ordered U_{HA} below the critical breakdown potential, even at a given electrolyte.[25] Exemplified by 0.3 M oxalic acid (Figure 3), we can obtain the conical OTNPAs with tunable periods: 260 nm (U_{HA} = 120 V), 280 nm (U_{HA} = 130 V), 290 nm (U_{HA} = 140 V) and 350 nm (U_{HA} = 160 V). With the U_{HA} increasing, the long-range ordering of the in situ grown conical nanopores becomes better, evidently seen from their SEM top-views (Figure 3 and Figure 1c$_1$). Note that burning events frequently occur as U_{HA} = 160 V, whereas the long-range ordering becomes poor as the U_{HA} drops to 120 V. In contrast, self-ordered nanopits with D_{int} of 70−120 nm can be obtained in 0.3 M sulfuric acid, where self-ordered U_{HA} falls in the range of 40−70 V (see Figure S3 in the Supporting Information). This is because lower U_{HA} can generate higher current density in the sulfuric acid system (e.g., the peak current density can arrive at 100 mA/cm^2 when anodizing at 40 V).[28] Clearly, controlling the appropriate current density in the HA regime is very crucial to achieve the long-range ordering growth of nanopores.[25]

As for a given U_{HA}, the current density can be tuned by adding other electrolytes in oxalic acid system,[29] which is an effective way to improve the long-range ordering of nanopit patterns. For example, in pure oxalic acid system, it is impossible to obtain self-ordered nanopit pattern as U_{HA} = 110 V, as shown in Figure 4a. However, the regular nanopit patterns can be produced (Figure 4b) by simply adding a tiny quantity of sulfuric acid (C_{SA} = 0.015 M) into oxalic acid while keeping the anodizing voltage (110 V) and time (1.5 h) unchanged. Compared with the pure oxalic acid, the mixed electrolyte can make the peak current density dramatically increase from 0.06 A/cm^2 up to 0.12 A/cm^2 (Figure 4c). The oxide growth rate in the mixture is far higher than that in the

dx.doi.org/10.1021/am301603e | ACS Appl. Mater. Interfaces 2012, 4, 5678−5683

pure acid, which is the reason of inducing the long-range ordering of pores. We suppose that the addition of tiny quantity of sulfuric acid can increase the ionic conduction of the electrolyte so as to increase the current density at the same U_{HA}.[35]

By simply tuning the C_{SA}, we can obtain self-ordered nanopit patterns with interpore distances tunable in the range of 100−300 nm. The detailed investigations into the effects of C_{SA} on the self- ordered U_{HA} and resultant D_{int} are shown in Table S1 and Figure S4 in the Supporting Information. Both the upper limit of self-ordered U_{HA} values and their tunable range gradually decrease with the C_{SA} increasing. The magnitude of D_{int} can be simultaneously influenced by both C_{SA} and U_{HA}. To deeply understand the relationship among the three parameters (C_{SA}, U_{HA}, and D_{int}) and grasp the ability to tailor the period, we gave the curve of the maximum U_{HA} as a function of C_{SA} (Figure 4d) and the curve of D_{int} as a function of U_{HA} (Figure 4e), respectively. Here, the data acquisition is simplified according to general knowledge that the optimal arrangement of self-ordered nanopores occurs at the maximum U_{HA}. As a result, a second order exponential decay curve can be fitted in Figure 4d as the following equation, $U_{HA} = 73.8 + 18.1e^{-C_{SA}/0.0014} + 58.4e^{-C_{SA}/0.0300}$. Meantime, the periods linearly vary with the U_{HA}, obeying the equation $D_{int} = 3.2U_{HA} - 147.43$. That is, to tailor the desired periods (e.g., 130 and 236 nm) of regular nanopit patterns, we may calculate the required C_{SA} to be 0.045 and 0.007 M and the U_{HA} to be 87 and 120 V. Figure 4f shows the two samples as-prepared at the corresponding reaction conditions. The experimentally measured D_{int} values are 128.5 ± 5.1 nm and 238.1 ± 8.2 nm, respectively, which agree well with the predefined periods.

Besides, the stable HA reactions can be realized at 160 V and even bigger voltages by simply adding ethanol into the oxalic acid system, which may be ascribed to enhanced heat dissipation and reduced ionic conduction.[30] As shown in Figure 5a, the peak current density can dramatically decrease from 200 mA/cm^2 down to 60 mA/cm^2 and then the current−time transient presents a nearly exponential decrease as a function of time, rather than an abnormal fluctuation. The optical images of the samples as-prepared before and after adding ethanol are displayed in the insets of Figure 5a. Clearly, the latter shows uniformly light yellow at the whole area while the former becomes tan-yellow at the local due to the occurrence of burning events. Note that, despite having the same anodizing time (1.5 h), the ordering degree of the sample (Figure 5b) formed in the mixed electrolyte is not as good as that formed in the pure oxalic acid (Figure 3d). This may be ascribed to the greatly reduced current density and oxide growth rate. In this case, the sustainable maximum U_{HA} can arrive at 180 V, above which the Al foils would be burnt. Figure 5b−d shows typical nanopit patterns obtained at 160, 170, and 180 V for 3 h. With the U_{HA} increasing, the regularity of nanopit patterns becomes better. Similar phenomena can also be observed as extending the anodizing time (e.g., from 0.5 to 6 h) at the given voltages (see Figure S5 in the Supporting Information). All samples own perfect long-range ordering with domain sizes above 3.5 μm as the anodizing time reaches 6 h.

Figure 6a lists the dependence of the D_{int} of self-ordered nanopits on the matched U_{HA} under different electrolyte systems. The details are as follows: (1) sulfuric acid at 40−70 V for D_{int} = 70−120 nm, with PC = 1.18 nm/V; 2) oxalic acid at 120−150 V for D_{int} = 260−320 nm, with PC = 2.2 nm/V; (3) a mixture of oxalic and sulfuric acid at 80−140 V for D_{int} = 100−300 nm, with PC = 3.2 nm/V; (4) a mixture of oxalic acid and ethanol at 160−180 V for D_{int} = 330−370 nm, with PC = 2.2 nm/V. Accordingly, we can easily obtain desired OTNPAs with periods of 70−370 nm. Figure 6b shows several representative

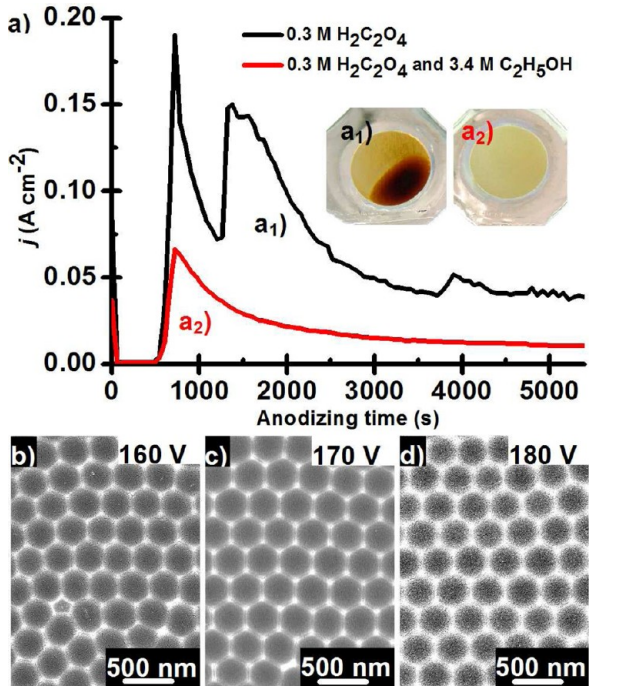

Figure 5. (a) Current−time transients during the hard anodizing of electro-polished aluminum foils in the $H_2C_2O_4$ (marked as "a_1") and $H_2C_2O_4$−C_2H_5OH mixture (marked as "a_2") at 160 V. The optical images of their corresponding samples are shown in the inset for the contrast. b-d) SEM images of self-ordered nanopit patterns generated at the anodizing voltage of 160 V, 170 and 180 V, respectively.

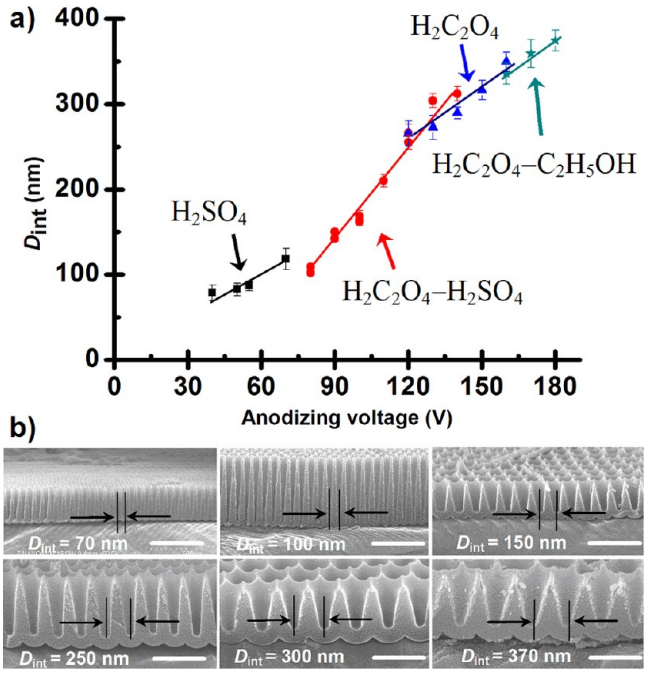

Figure 6. 3D OTNPA structures with tunable periods. (a) Periods D_{int} as a function of anodizing voltages under varied electrolytes. (b) SEM side-views of typical conical nanopores with tailored periods: 70, 100, 150, 250, 300, and 370 nm. Scale bars: 500 nm.

dx.doi.org/10.1021/am301603e | ACS Appl. Mater. Interfaces 2012, 4, 5678−5683

examples of OTNPA structures with the tailored periods of 70, 100, 150, 250, 300, and 370 nm, respectively. Note that the proportionality constant of the HA under different electrolytes varies with the electrolyte type and their divergence with the empirical value (2.0 nm/V) does not influence the in situ growth of taper-nanopores because the template-assisted growth of taper-nanopores is not so sensitive to the change of U_{MA} in the near zone.[24] Besides, to obtain high-quality OTNPA structures, dilute phosphoric acid and oxalic acid are used as the anodizing electrolyte at the MS-MA-EW stage as $D_{int} > 100$ nm and $D_{int} \leq 100$ nm, respectively.

CONCLUSIONS

A powerful nanofabrication method based on the combined OS-HA-EP and MS-MA-EW has been successfully proposed for the controllable tailoring of the 3D OTNPA structures. The basic tailoring principles and relationships between the geometrical parameters and reaction conditions have been well revealed. Compared with those methods reported previously, this method of using the combination of pure chemical nanofabrication technologies has many appealing advantages: (1) it can independently control the structural parameters of 3D taper-nanopores such as profiles and periods at one's own will, unachievable by any conventional single top-down and bottom-up nanofabrication technique; (2) the periods of taper-nanopores reported here can satisfy most research demand and can also be further broadened; (3) the required electrochemical equipments are very simple, cheap and available to most researchers; (4) it can obtain large-area (e.g., centimeter-scale) samples at a low cost; (5) it is industry-compatible and thus very promising to evolve into be a real practical nanofabrication technique. The remarkable nanofabrication ability reported here opens a door for exploring the novel physical and chemical properties of different materials of 3D nanotaper arrays.

ASSOCIATED CONTENT

Supporting Information

Two groups of contrast SEM images showing the rapid fabrication ability of the OS-HA-EP over the OS-MA-EP; optical photo of a 2-in. sample; current−time transient during HA of Al foils in H_2SO_4 at 40 V and the as-prepared nanopit patterns with tunable periods; average interpore distances of nanopit patterns obtained under different anodizing voltages in oxalic acid mixed with different concentrations of H_2SO_4; SEM images of representative nanopit patterns obtained in the mixed $H_2C_2O_4$ and H_2SO_4; detailed data showing the effects of anodizing voltages and durations to the self-organized growth of nanopits in the mixed oxalic acid and ethanol. This material is available free of charge via the Internet at http://pubs.acs.org.

AUTHOR INFORMATION

Corresponding Author

*E-mail: xfgao2007@sinano.ac.cn.

Notes

The authors declare no competing financial interest.

ACKNOWLEDGMENTS

This work was supported by National Basic Research Program of China (2012CB933200, 2009CB930802), National Natural Science Foundation of China (50973081, 91023003, 21104093), and the Key Research Program of Chinese Academy of Sciences (KJZD-EW-M01).

REFERENCES

(1) Parker, A. R.; Townley, H. E. *Nat. Nanotechnol.* **2007**, *2*, 347.
(2) Gao, X.; Yan, X.; Yao, X.; Xu, L.; Zhang, K.; Zhang, J.; Yang, B.; Jiang, L. *Adv. Mater.* **2007**, *19*, 2213.
(3) Choi, K.; Park, S. H.; Song, Y. M.; Lee, Y. T.; Hwangbo, C. K.; Yang, H.; Lee, H. S. *Adv. Mater.* **2010**, *22*, 3713.
(4) Liu, K.; Yao, X.; Jiang, L. *Chem. Soc. Rev.* **2010**, *39*, 3240.
(5) Yanagishita, T.; Yasui, K.; Kondo, T.; Kawamoto, Y.; Nishio, K.; Masuda, H. *Chem. Lett.* **2007**, *36*, 530.
(6) Yanagishita, T.; Kondo, T.; Nishio, K.; Masuda, H. *J. Vac. Sci. Technol. B* **2008**, *26*, 1856.
(7) Xu, J.; Lavan, D. A. *Nat. Nanotechnol.* **2008**, *3*, 666.
(8) Sparreboom, W.; van den Berg, A.; Eijkel, J. C. T. *Nat. Nanotechnol.* **2009**, *4*, 713.
(9) Hou, X.; Guo, W.; Jiang, L. *Chem. Soc. Rev.* **2011**, *40*, 2385.
(10) Zhou, Y.; Guo, W.; Cheng, J.; Liu, Y.; Li, J.; Jiang, L. *Adv. Mater.* **2012**, *24*, 962.
(11) Zhao, S.; Roberge, H.; Yelon, A.; Veres, T. *J. Am. Chem. Soc.* **2006**, *128*, 12352.
(12) Yamauchi, Y.; Wang, L.; Ataee-Esfahani, H.; Fukata, N.; Nagaura, T.; Inoue, S. *J. Nanosci. Nanotechnol.* **2010**, *10*, 4384.
(13) Yamauchi, Y.; Nagaura, T.; Ishikawa, A.; Chikyow, T.; Inoue, S. *J. Am. Chem. Soc.* **2008**, *130*, 10165.
(14) Yamauchi, Y.; Nagaura, T.; Inoue, S. *Chem.−Asian J.* **2009**, *4*, 1059.
(15) Yamauchi, Y.; Suzuki, N.; Radhakrishnan, L.; Wang, L. *Chem. Rec.* **2009**, *9*, 321.
(16) Wu, K. C.-W.; Jiang, X.; Yamauchi, Y. *J. Mater. Chem.* **2011**, *21*, 8394.
(17) Nagaura, T.; Takeuchi, F.; Yamauchi, Y.; Wada, K.; Inoue, S. *Electrochem. Commun.* **2008**, *10*, 681.
(18) LeClere, D. J.; Thompson, G. E.; Derby, B. *Nanotechnology* **2009**, *20*, 245304.
(19) Yamauchi, Y.; Nagaura, T.; Takai, K.; Suzuki, N.; Sato, K.; Fukata, N.; Inoue, S.; Kishimoto, S. *J. Phys. Chem. C* **2009**, *113*, 9632.
(20) Yanagishita, T.; Endo, T.; Yamaguchi, Y.; Nishio, K.; Masuda, H. *Chem. Lett.* **2009**, *38*, 274.
(21) Yanagishita, T.; Nishio, K.; Masuda, H. *Appl. Phys. Exp.* **2008**, *1*, 067004.
(22) Yanagishita, T.; Endo, T.; Nishio, K.; Masuda, H. *Jpn. J. Appl. Phys.* **2010**, *49*, 065202.
(23) Masuda, H.; Yamada, H.; Satoh, M.; Asoh, H.; Nakao, M.; Tamamura, T. *Appl. Phys. Lett.* **1997**, *71*, 2770.
(24) Li, C.; Li, J.; Chen, C.; Gao, X. *Chem.Commun.* **2012**, *48*, 5100.
(25) Lee, W.; Ji, R.; Gösele, U.; Nielsch, K. *Nat. Mater.* **2006**, *5*, 741.
(26) Chu, S.-Z.; Wada, K.; Inoue, S.; Isogai, M.; Yasumori, A. *Adv. Mater.* **2005**, *17*, 2115.
(27) Ono, S.; Saito, M.; Asoh, H. *Electrochim. Acta* **2005**, *51*, 827.
(28) Schwirn, K.; Lee, W.; Hillebrand, R.; Steinhart, M.; Nielsch, K.; Gösele, U. *ACS Nano* **2008**, *2*, 302.
(29) Kashi, M. A.; Ramazani, A.; Noormohammadi, M.; Zarei, M.; Marashi, P. *J. Phys. D: Appl. Phys.* **2007**, *40*, 7032.
(30) Li, Y. B.; Zheng, M. J.; Ma, L. *Appl. Phys. Lett.* **2007**, *91*, 073109.
(31) Santos, A.; Montero-Moreno, J. M.; Bachmann, J.; Nielsch, K.; Formentín, P.; Ferré-Borrull, J.; Pallarès, J.; Marsal, L. F. *ACS Appl. Mater. Interfaces* **2011**, *3*, 1925.
(32) Masuda, H.; Fukuda, K. *Science* **1995**, *268*, 1466.
(33) Li, A. P.; Müller, F.; Birner, A.; Nielsch, K.; Gösele, U. *J. Appl. Phys.* **1998**, *84*, 6023.
(34) Li, J.; Li, C.; Gao, X. *Appl. Surf. Sci.* **2011**, *257*, 10390.
(35) Thompson, G. E.; Wood, G. C. *Nature* **1981**, *290*, 230.